ADVANCES IN ATMOSPHERIC SCIENCES, VOL. 31, MARCH 2014, 283–292

Simulated Spatial Distribution and Seasonal Variation of Atmospheric Methane over China: Contributions from Key Sources

ZHANG Dingyuan[1,2], LIAO Hong[*1], and WANG Yuesi[1]

[1]*State Key Laboratory of Atmospheric Boundary Layer Physics and Atmospheric Chemistry, Institute of Atmospheric Physics, Chinese Academy of Sciences, Beijing* 100029
[2]*University of Chinese Academy of Sciences, Beijing* 100049

(Received 22 January 2013; revised 18 May 2013; accepted 21 May 2013)

ABSTRACT

We used the global atmospheric chemical transport model, GEOS-Chem, to simulate the spatial distribution and seasonal variation of surface-layer methane (CH_4) in 2004, and quantify the impacts of individual domestic sources and foreign transport on CH_4 concentrations over China. Simulated surface-layer CH_4 concentrations over China exhibit maximum concentrations in summer and minimum concentrations in spring. The annual mean CH_4 concentrations range from 1800 ppb over western China to 2300 ppb over the more populated eastern China. Foreign emissions were found to have large impacts on CH_4 concentrations over China, contributing to about 85% of the CH_4 concentrations over western China and about 80% of those over eastern China. The tagged simulation results showed that coal mining, livestock, and waste are the dominant domestic contributors to CH_4 concentrations over China, accounting for 36%, 18%, and 16%, respectively, of the annual and national mean increase in CH_4 concentration from all domestic emissions. Emissions from rice cultivation were found to make the largest contributions to CH_4 concentrations over China in the summer, which is the key factor that leads to the maximum seasonal mean CH_4 concentrations in summer.

Key words: methane, GEOS-Chem, seasonal variation, foreign and domestic contributions

Citation: Zhang, D. Y., H, Liao, and Y. S. Wang, 2014: Simulated spatial distribution and seasonal variation of atmospheric methane over China: Contributions from key sources. *Adv. Atmos. Sci.*, **31**(2), 283–292, doi: 10.1007/s00376-013-3018-y.

1. Introduction

As a long-lived anthropogenic greenhouse gas, second only to CO_2, methane (CH_4) influences the radiative balance of the Earth (IPCC, 2007). Methane also plays a critical role in atmospheric chemistry by affecting the oxidizing capacity of the atmosphere (Fiore et al., 2002; Wang et al., 2004). Consequently, it is important to get a clear understanding of the concentrations and seasonal variations of atmospheric CH_4, especially for China where both air quality and climate change are of great concern.

Atmospheric CH_4 comes from anthropogenic and natural emissions, and it decays by a photochemical reaction with hydroxyl radical (OH) in the troposphere, biological CH_4 oxidation in soil, and chemical reactions with Cl and O in the stratosphere, leading to the long lifetime of 8.7 ± 1.3 years (IPCC, 2007). Major anthropogenic CH_4 sources in China include coal mining, oil and gas processing, livestock, rice cultivation, landfill, biomass burning, and biofuel. Major natural CH_4 sources in China include wetlands and termites. Quite a number of studies have attempted to understand the concentrations, distributions, and seasonal variations of CH_4 over China. Ground-based measurements in China have shown that the concentrations of atmospheric CH_4 are highly variable from site to site (in the range of 1700–2400 ppb) and suggested that both the magnitude and seasonal variation of CH_4 are influenced by local anthropogenic sources and transport from the surrounding regions (Wang and Wang, 2000; Zhou et al., 2004; Liu et al., 2009; Fang et al., 2012). Satellite observations have good spatial and temporal coverage of CH_4. Methane concentrations in the mid-upper troposphere of China measured by the Atmospheric Infrared Sounder (AIRS) on Aqua have shown that CH_4 concentrations are highest in summer (Zhang et al., 2011a). The column-averaged volume mixing ratios of CH_4 from the Scanning Imaging Absorption Spectrometer for Atmospheric Chartography (SCIAMACHY) on Envisat have also shown maximum values in summer for China (Frankenberg et al., 2006). On an annual mean basis, measurements by SCIAMACHY have indicated that CH_4 mixing ratios are highest in southeastern China and lowest in the Qinghai–Tibet Plateau (Zhang et al., 2011b). However, satellite observations cannot explain the mechanism of these spatiotemporal variations and explicitly distinguish the contributions to atmospheric CH_4 concentrations from different sources and regions of emissions. Al-

* Corresponding author: LIAO Hong
Email: hongliao@mail.iap.ac.cn

though quite a number of studies have attempted to quantify CH_4 emissions from different sectors (Yan et al., 2003; Ding et al., 2004; Zhou et al., 2007a), these studies did not examine the contributions from each domestic source to concentrations of atmospheric CH_4. Fraser et al. (2011) investigated the relative contributions of local emissions and long-range transport to Australian CH_4 using the GEOS-Chem chemistry transport model. However, to our knowledge, no such work has been done for CH_4 concentrations over China.

In the present reported study we examined the spatial and temporal variations of atmospheric CH_4 over China and quantified the impacts of individual domestic sources and overseas transport on the concentrations of CH_4, using the global three-dimensional chemical transport model, GEOS-Chem. The model is described in section 2. Section 3 presents the results of simulated methane concentrations over China and an evaluation of the model. In section 4 we analyze the contribution to concentrations of CH_4 over China from foreign emissions and transport. And finally, in section 5, we discuss the contributions from various domestic sources to surface-layer CH_4 over China.

2. Model description and experiments

2.1. *GEOS-Chem Model*

The GEOS-Chem model is a global three-dimensional chemical transport model driven by the GEOS-5 assimilated meteorological data from the Goddard Earth Observing System (GEOS) at the National Aeronautics and Space Administration (NASA) Global Modeling and Assimilation Office (GMAO).We used the model (v8-03-02, available online at http://acmg.seas.harvard.edu/geos/) with a horizontal resolution of 2° (lat) $\times 2.5^\circ$ (lon) and 47 vertical layers up to 0.01 hPa. The model simulates CH_4 from emissions sources, the removal of CH_4 due to reaction with OH in the troposphere, loss in the stratosphere, and a soil sink, which were implemented in the GEOS-Chem by Duncan et al. (2000) and Wang et al. (2004). There are ten tagged tracers for CH_4 concentrations from each of the CH_4 sources and one tracer for the total CH_4. The relevant methane sources are shown in Table 1.

The global three-dimensional monthly mean tropospheric OH concentrations were taken from a full chemistry O_x–NO_x–VOC simulation of the GEOS-Chem model (Fiore et al., 2003). The lifetime of methyl chloroform (CH_3CCl_3) against oxidation by OH was 5.1 years, which is within the range of 4.6–5.2 years estimated by Prinn et al. (2005). The decay of CH_4 in the stratosphere was treated as described in Wang et al. (2004). The GEOS-Chem simulation of CH_4 has been used to examine the Asian and European sources of CH_4 from CH_4–C_2H_6–CO correlations in Asian outflow (Xiao et al., 2004), to analyze the changes in CH_4 growth rate from 1988 to 1997 (Wang et al., 2004), and to investigate the Australian CH_4 budget (Fraser et al., 2011).

2.2. *Emissions*

Anthropogenic CH_4 emissions from coal mining, gas and oil processing, livestock and waste were from the Emission Database for Global Atmospheric Research (EDGAR v4.0, 2009) inventory, which are constant throughout the year. Monthly emissions of CH_4 from biomass burning were taken from the Global Fire Emissions Database (GFED v2) inventory (van der Werf et al., 2006). Biofuel emissions of CH_4 were taken from Yevich and Logan (2003), which do not have seasonal variations. Rice emissions from EDGAR v4.0 were scaled monthly based on soil wetness, and were updated for China following Yan et al. (2003). Natural emissions from wetlands vary monthly, as described by Pickett-Heaps et al. (2011). Natural emissions from termites were included, and soil absorption was treated as a sink (Fung et al., 1991), both of which were assumed to be constant throughout the year. The global total emissions and emissions over China are listed in Table 1. For 2004, the global total emission of CH_4 was 522.9 Tg, of which the major sources were wetlands, livestock, gas and oil, and waste, which accounted for 31.7%, 20.4%, 13.7%, and 12.2% of the global total emission, respectively. The total emission of CH_4 in China was 63.0 Tg, of which the major sources were coal mining (32.7%), rice cultivation (21.1%), livestock (18.0%), and waste (15.2%).

Table 1. Global and Chinese CH_4 emissions for 2004.

Source ($Tgyr^{-1}$)	Global	(%)[a]	China	(%)[b]
Gas and oil	71.45	13.7	1.87	3.0
Coal	34.97	6.7	20.57	32.7
Livestock	106.86	20.4	11.34	18.0
Waste	63.73	12.2	9.55	15.2
Biofuel	12.49	2.4	3.3	5.2
Rice	33.57	6.4	13.27	21.1
Other anthropogenic	1.55	0.3	0.24	0.4
Biomass burning	20.25	3.9	0.35	0.6
Wetlands	165.94	31.7	1.78	2.8
Termites	12.05	2.3	0.72	1.1
Total	522.86	100.0	62.99	100.0

[a] Percentage of individual source in global total emission.

[b] Percentage of individual source in Chinese total emission.

The total emission in China was 12% of the global total CH_4 emission.

2.3. *Numerical experiments*

For the purpose of investigating the spatial distribution and seasonal variation of CH_4 and quantifying the impacts of domestic sources and foreign transport on CH_4 concentrations over China, we performed the following simulations using the GEOS-Chem:

(1) Standard simulation (STAND): Global simulation of CH_4 for 2004, with the initial global methane fields for 1 January 2004 obtained from A. Fraser (2011, personal communication).

(2) To investigate the contributions of foreign emissions to CH_4 concentrations over China, we performed two 20-yr simulations of CH_4. One simulation considered global emissions of CH_4 (referred to as CTRL) and the other simulation considered foreign emissions only (referred to as FC). The initial fields of methane were set to zero globally for these two simulations. The ratios of average concentrations in the last five years in FC to those in CTRL represent the contributions of foreign emissions to CH_4 concentrations over China. Since CH_4 is a long-lived gas, the 20-yr integration allowed CH_4 in the final years of the simulation to reach a quasi-equilibrium state.

(3) Tagged simulation: To quantify the impacts of each domestic source on CH_4 concentrations over China, we performed a tagged simulation for each of ten CH_4 sources. The tagged simulation considered Chinese CH_4 emissions only, and all tracers were set to zero at the beginning of every month, which reset the influence of emissions from month to month, so that the CH_4 concentrations of the tagged tracers clearly accounted for the monthly contributions from individual CH_4 sources over China. These concentrations were only a small fraction of the total CH_4. The tagged simulation was driven by the 2004 meteorological fields.

3. Simulated CH_4 over China and model evaluation

3.1. *Simulated spatial distributions and seasonal variations*

The seasonal mean concentrations of surface-layer CH_4 simulated in STAND for 2004 are shown in Fig. 1. The model results show maximum concentrations in summer and minimum concentrations in spring. In summer, the largest CH_4 concentrations that exceed 2300 ppb are simulated over eastern (east of 110°E) and southeastern China, as a result of the increases in biogenic emissions from rice with temperature during the growing period of rice. The combination of weak surface sources and a stronger OH sink relative to winter (Su et al., 2012) leads to the lowest CH_4 concentrations in spring. The minimum CH_4 concentrations below 1800 ppb

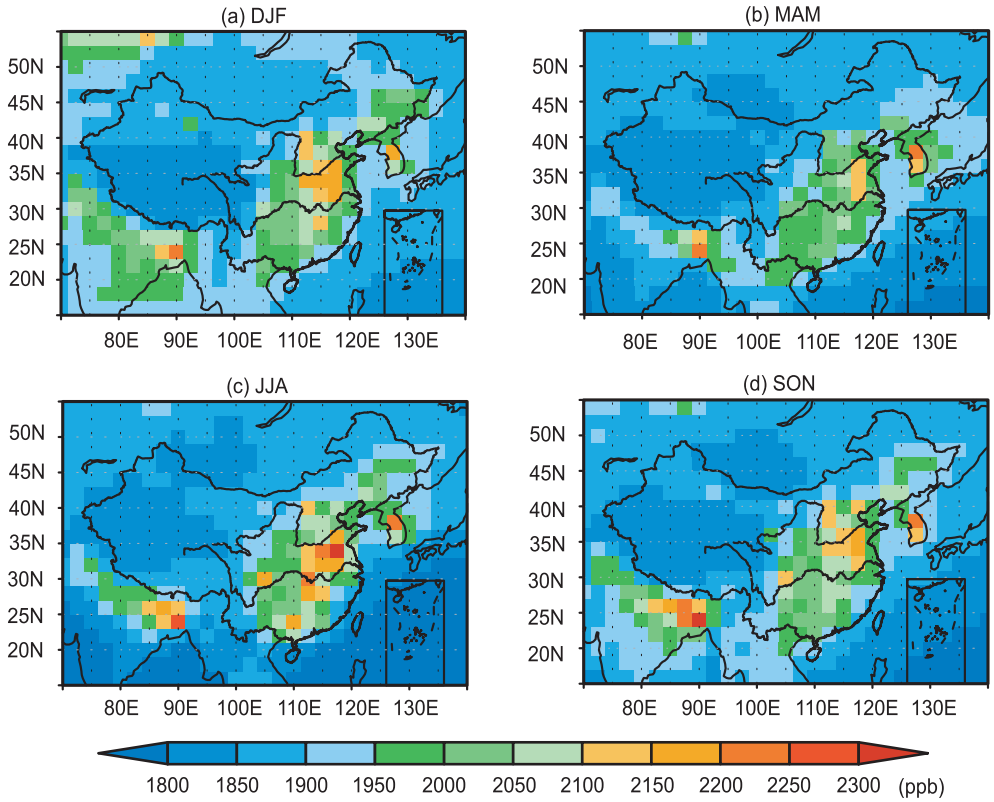

Fig. 1. Simulated seasonal mean concentrations of surface-layer CH_4 for 2004: (a) winter (DJF); (b) spring (MAM); (c) summer (JJA); (d) fall (SON).

are found over the Tibetan Plateau. This simulated seasonality is consistent with the observed seasonal variation in China from satellites in the studies of Frankenberg et al. (2006) and Schneising et al. (2009).

It can also be seen from Fig. 1 that the concentrations of CH_4 over eastern China are much higher than those over western (west of 110°E) China throughout the year. This regional pattern of CH_4 reflects the influence of anthropogenic emissions from the more populated eastern China. The simulated contributions from human activities to atmospheric CH_4 concentrations range from 200 ppb to 400 ppb, consistent with the magnitude obtained from measurements. The average measured concentration of CH_4 during 2003–2005 was 2120 ± 150 ppb at Taihu station located in eastern China (Ji et al., 2006) and the average measured CH_4 during 1991–2004 was 1814 ± 47 ppb at Waliguan station located in western China (Zhou et al., 2007b).

Figure 2 shows the simulated seasonal mean vertical distributions of CH_4 along the latitude of 35°N in China. A strong enhancement of the CH_4 plume is found from the surface to about 10 km altitude along this latitude over 70°–140°E in summer, which agrees with that observed by AIRS and modeled by TM3 in Xiong et al. (2009). Their study suggested that the enhancement is associated with the increasing local emissions and the strong transport of CH_4 from the lower to the upper troposphere during the monsoon season. It should be noted that the enhancement over 120°–130°E is also very strong, which is from South Korea, as shown in Fig. 1.

3.2. *Model evaluation*

We focus here on the simulated monthly mean concentrations for 2004 from the standard simulation. Surface and aircraft datasets were used to help assess how well the model reproduced the observed seasonality and vertical profiles of CH_4 in the troposphere.

3.2.1. *Concentrations of CH_4 from global background monitoring stations*

Six representative ground-based flask monitoring stations from the NOAA Earth System Research Laboratory (ESRL) (Dlugokencky et al., 2012) network, known to be little-influenced by local emissions, were chosen according to the latitudinal representation as shown in Fig. 3: Alert in the Arctic, Trinidad Head in the Northern Hemisphere mid-latitudes, Mauna Loa in the Northern Hemisphere tropics, Cape Matatula in the Southern Hemisphere tropics, Cape Grim in the Southern Hemisphere mid-latitudes, and South Pole in the Antarctic.

Figure 4 compares the simulated with observed monthly mean concentrations of CH_4 at these sites for 2004. It can be seen that the monthly mean CH_4 concentrations from observations generally have a maximum in January, March, and April and a minimum in July and August in the Northern

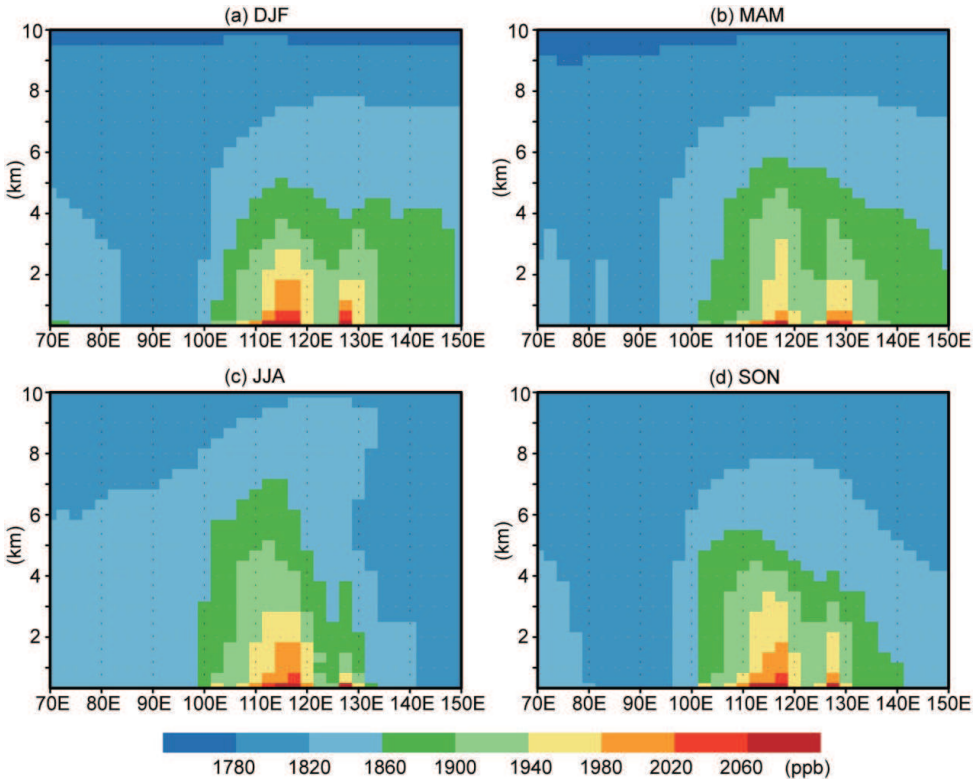

Fig. 2. Simulated seasonal mean vertical distributions of CH_4 for 2004 in China; (a) winter (DJF); (b) spring (MAM); (c) summer (JJA); (d) fall (SON).

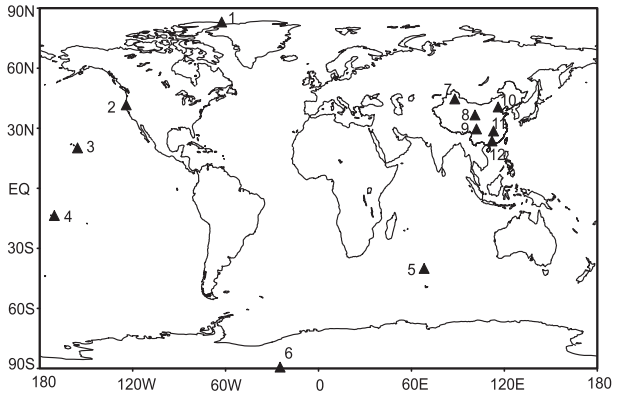

Fig. 3. Locations of observational data used in this study. The black triangles represent 12 sites: (1) Alert; (2) Trinidad Head; (3) Mauna Loa; (4) Cape Matatula; (5) Cape Grim; (6) South Pole; (7) Fukang; (8) Waliguan; (9) Gongga Mountain; (10) Beijing; (11) Changsha; (12) Dinghu Mountain.

Hemisphere; and those in the Southern Hemisphere show a maximum in July and September and a minimum in February and March. The model captures the magnitude and seasonal cycle of the observed CH_4 concentrations at all sites except for Alert. Modeled CH_4 concentrations at Alert show smaller seasonal variations compared to the measurements. The model also tends to underestimate CH_4 concentrations at Alert and Trinidad Head. The underestimates in sites between 30°N and 90°N were also found in the version of the GEOS-Chem model used by Xiao et al. (2004). The model results show high correlations with observations, with correlation coefficients in the range of 0.84–0.99 at all stations. Table 2 presents a summary of the statistics of comparisons of the simulated concentrations of CH_4 with measurements for individual sites. The mean biases (MBs) of the background sites range from −9.23 to 8.33 ppb, and the normalized mean biases (NMBs) of these sites range from −0.50% to 0.47%.

The fairly good agreement between the model results and the observations gave us confidence for studying the impact of foreign emissions on concentrations of CH_4 over China.

3.2.2. *Concentrations of CH_4 at sites in China*

Since CH_4 is a long-lived gas, we compared the simulated monthly mean concentrations with multi-year averages of measured concentrations for six representative surface sites in China. Three urban sites represented fast-developing regions in eastern China: Dinghu Mountain (23°N, 112°E) in the Pearl River Delta region, Changsha (28°N, 113°E) in the Lake Dongting watershed, and Beijing in the North China Plain (40°N, 116°E). Three rural sites represented underde-

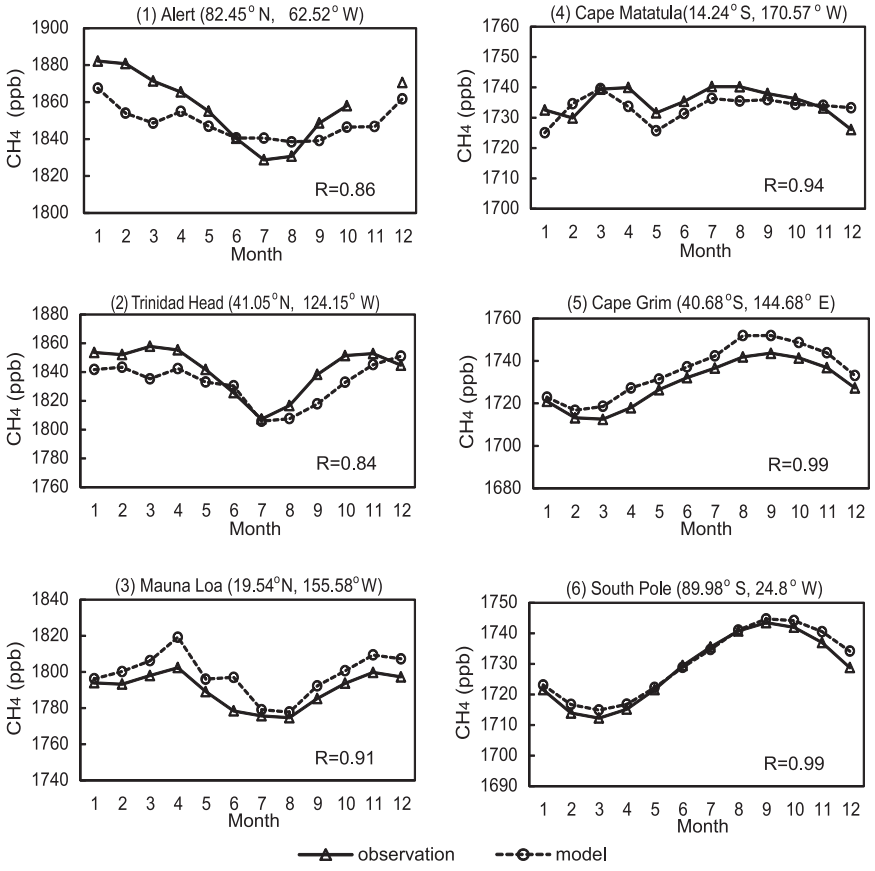

Fig. 4. Comparisons of monthly mean CH_4 mixing ratios from observations and those from the standard simulation at the background sites for 2004. *R* values are the correlation coefficient between observations and model results.

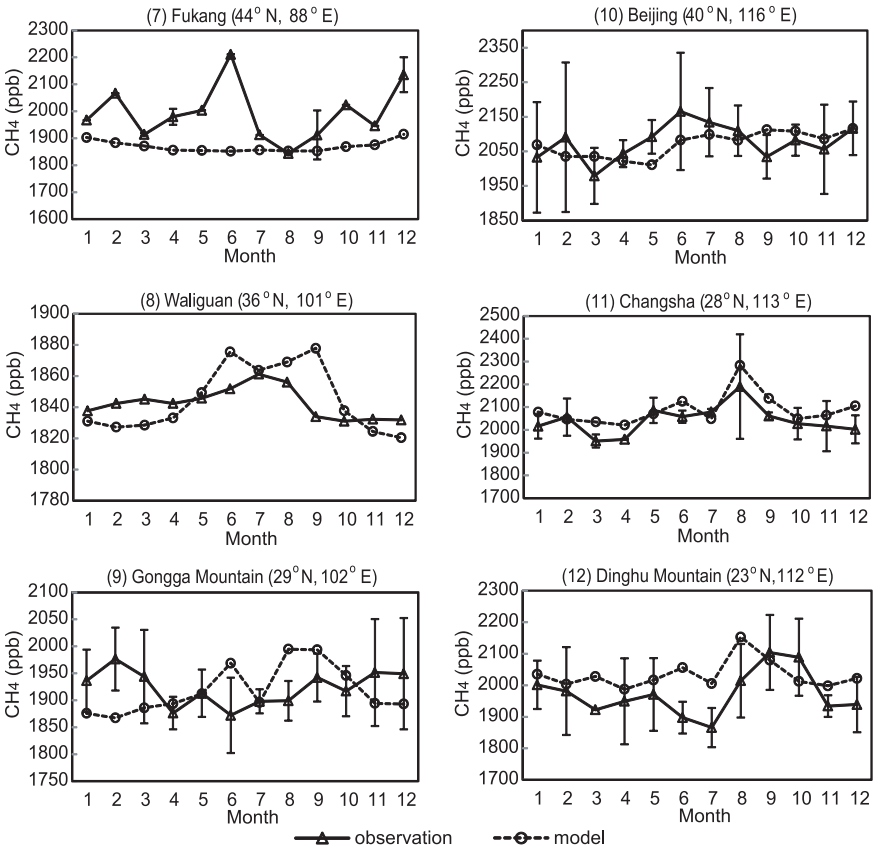

Fig. 5. Comparisons of monthly mean CH_4 mixing ratios from observations (error bars indicate one standard deviation) and those from the standard simulation at Chinese sites. Time periods of observations: Dinghu Mountain (2006–08); Changsha (2009–10); Gongga Mountain (2005–10); Waliguan (2004); Beijing (2005–07); Fukang (2009–10).

veloped inland regions in western China: Gongga Mountain (29°N, 102°E) in the southwest mountain area, Waliguan (36°N, 101°E) in the Tibetan Plateau, and Fukang (44°N, 88°E) in the Junggar basin. Measurements at all the sites except those at Waliguan were automatic continuous measurements taken using the gas chromatograph as described in Wang and Wang (2003), and the observed values for Waliguan were taken from ESRL/NOAA (Dlugokencky et al., 2012).

Figure 5 compares the simulated monthly mean concentrations of surface-layer CH_4 with observations. The simulated CH_4 concentrations capture the general feature of observed high CH_4 concentrations in summer or autumn at Waliguan, Beijing, Changsha, and Dinghu Mountain, but do not reproduce the seasonal variations at Fukang and Gongga Mountain. At Fukang, a remote site in northwestern China, CH_4 concentrations are underestimated by the model. While the observed concentrations show a maximum in June and a minimum in August, the simulated concentrations show small seasonal variability. At Gongga Mountain, the simulated seasonal cycle is out of phase with the observed one. At Waliguan, the observed CH_4 concentrations peak in July and the modeled CH_4 concentrations have two peaks in June and September. At Beijing, the observed CH_4 concentrations show a minimum in March but the simulated minimum occurs two months later. The model has a relatively better performance in simulating the seasonal variations at Changsha and Dinghu Mountain. At these sites, the MBs range from −122.82 to 60.37 ppb and the NMBs range from −6.16% to 3.08% (Table 2), which are larger than the MBs and NMBs at the foreign background sites discussed above. The large biases in simulated CH_4 concentrations in China can mainly be attributed to the representation of local emissions in the model (Wang et al., 2004). It should be mentioned that the discrepancies at these Chinese sites may partly be caused by the fact that the model results are for 2004 and the measurements were made in different years.

3.2.3. *Vertical profiles of CH_4 in spring outflow from China*

The Transport and Chemical Evolution over the Pacific (TRACE-P) aircraft mission was conducted in February to April 2001 by the NASA Global Tropospheric Experiment (GTE) to observe the chemical outflow from Asia to the Pacific (Jacob et al., 2003). The measurements have been used to evaluate the simulated CH_4 in the earlier version of the GEOS-Chem model by Xiao et al. (2004), in which the model reproduced the observed vertical gradient with a positive bias in the boundary layer north of 30°N, owing to the high

Table 2. Summary of the statistics of comparisons of simulated concentrations of CH_4 with measurements.

No.	Sites	MB (ppb)	NMB (%)
1	Alert	−8.45	−0.46
2	Trinidad Head	−9.23	−0.50
3	Mauna Loa	8.33	0.47
4	Cape Matatula	−1.94	−0.11
5	Cape Grim	6.22	0.36
6	South Pole	1.72	0.10
7	Fukang	−122.82	−6.16
8	Waliguan	2.20	0.12
9	Gongga Moutain	−4.45	−0.23
10	Beijing	−6.51	−0.31
11	Changsha	47.09	2.31
12	Dinghu Moutain	60.73	3.08

Note: Mean bias (MB) = $1/N\sum_{i=1}^{N}(M_i - O_i)$, and normalized mean bias (NMB) = $100\% \times \sum_{i=1}^{N}(M_i - O_i)/\sum_{i=1}^{N} O_i$, where M_i is the model result at station i, O_i is the observed value at station i, and N is the number of model-observed pairs.

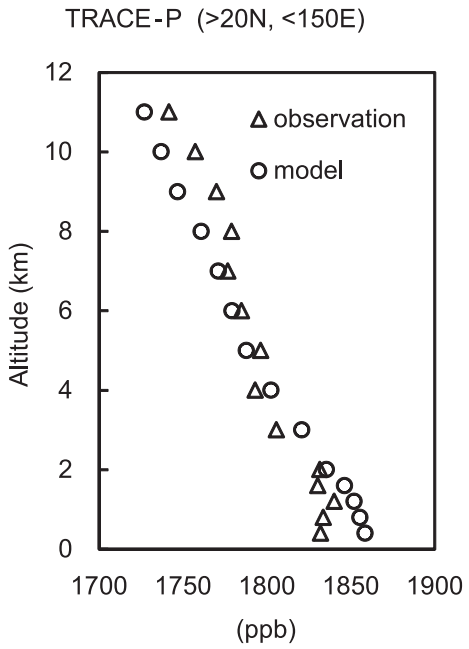

Fig. 6. Comparisons of the averaged vertical profile of CH_4 observed north of 20°N and west of 150° E during the TRACE-P aircraft mission and with model results. Observations are for 2001 and models are for 2004.

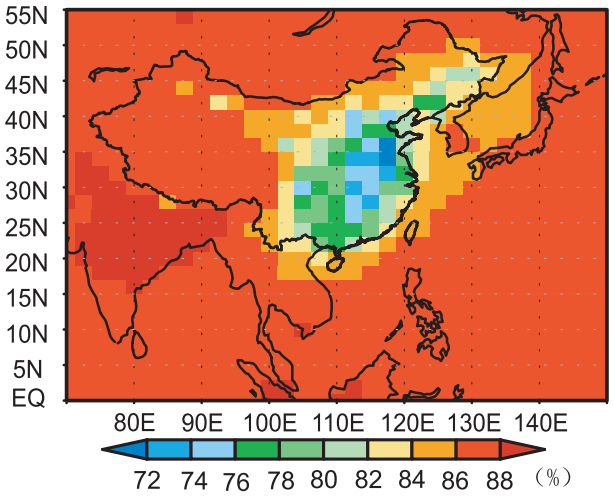

Fig. 7. Simulated spatial distribution of the ratios of annual mean surface-layer CH_4 concentrations in the last five years in FC to those in CTRL simulation.

livestock and landfill emissions of CH_4 from the Streets et al. (2003) inventory.

We focus our comparisons here on the mean vertical profiles of CH_4 concentrations in TRACE-P for a region north of 20°N and west of 150°E, with the averaged data obtained from flight number four to 20 of route DC-8 (http://www-gte.larc.nasa.gov/gte_mrg1.htm#TRACE-P). Note that the simulation was for 2004 and the TRACE-P observation was for 2001. The vertical profile of atmospheric CH_4 is not expected to vary significantly year by year since CH_4 is a long-lived gas. The model results were sampled along the flight tracks and were based on the standard simulation. As shown in Fig. 6, the vertical gradient and CH_4 mixing ratios throughout the troposphere are reasonably well reproduced by the model, with a positive bias of about 25 ppb below 1 km and a negative bias of about 20 ppb between 8 and 10 km.

4. Contributions to CH_4 concentrations over China as a result of foreign emissions

As described in section 2.3, the ratios of average CH_4 concentrations in the last five years in simulation FC to those in simulation CTRL represent the contributions of foreign emissions to CH_4 concentrations over China. Figure 7 shows the simulated spatial distribution of the ratios on an annual mean basis. A distinct feature is that the ratios are higher in western China and lower in eastern China. The largest ratio of over 86% is found over the Tibetan Plateau, reflecting the large contributions from foreign emissions and small local emissions in this region. The smallest ratio of 72% is simulated over eastern China around 35°N, indicating the relatively strong local sources from human activities.

Figure 8 presents the monthly variations in FC/CTRL ratios for western (west of 110°E) and eastern China (east of 110°E). The ratios in these two regions have similar seasonal variation. The ratio of FC/CTRL has a maximum of 86.0% in April and a minimum of 83.9% in August in western China, and it has a maximum of 82.4% in March and a minimum of 77.8% in August in eastern China. The peaks in March and April can be attributed to enhanced inflow from overseas (Holzer et al., 2005) and relatively weak local sources in these months. In August, as the domestic emissions from rice reach a maximum, the contributions of foreign emissions to CH_4 concentrations in China are the smallest.

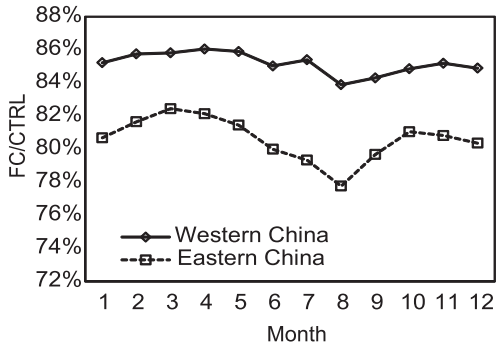

Fig. 8. The ratios of monthly average CH_4 concentrations in the last five years in FC to those in CTRL for eastern (east of 110°E) and western China (west of 110°E).

5. Contributions to CH_4 concentrations from each domestic source of emissions

Figure 9a shows the simulated monthly and national mean contributions of different domestic sources to surface-layer CH_4 concentrations over China, based on the tagged tracer simulation for 2004 (section 2.3). Averaged over the whole of China, emissions from coal mining, livestock, and waste lead to monthly increases in CH_4 concentrations of 19–35, 10–17, and 9–14 ppb, respectively, which account for 23%–47%, 11%–23%, and 10%–20% of the monthly contributions from all domestic emissions (MCADE), respectively. The contribution from rice cultivation is the largest in summer, accounting for about 47% of MCADE in August. Our model results show that biomass burning, biofuel, wetlands, and termites make small contributions to CH_4 concentrations over China.

Emissions from different sources influence the seasonal variation of CH_4. Contributions from individual domestic sources are the largest in winter and smallest in spring, except for emissions from rice, wetlands, and biomass burning. As the largest source (Zhang and Chen, 2010) in China, coal mining contributes to surface-layer CH_4 by up to 32 ppb in winter and by about 21 ppb in spring, reflecting mainly the seasonal variation of OH that leads to removal of CH_4, since coal mining emissions are constant throughout the year. Similarly, the contributions from emissions from livestock, waste, biofuel, and termites, exhibit the same seasonal variation. Emissions from rice cultivation dominate in summer with the maximum monthly contribution of 52 ppb to CH_4 concentrations, leading to the general pattern of the highest CH_4 concentrations in summer over eastern and southeastern China. The CH_4 emission occurs in the early phase of the rice growing season, and trails off as the rice matures (Shangguan et al., 1993). In the summer the temperature increases. Rice thrives in this hot weather and releases a burst of methane. Emissions from biomass burning make a small contribution to CH_4 concentration all year round; a relatively high value of 2 ppb

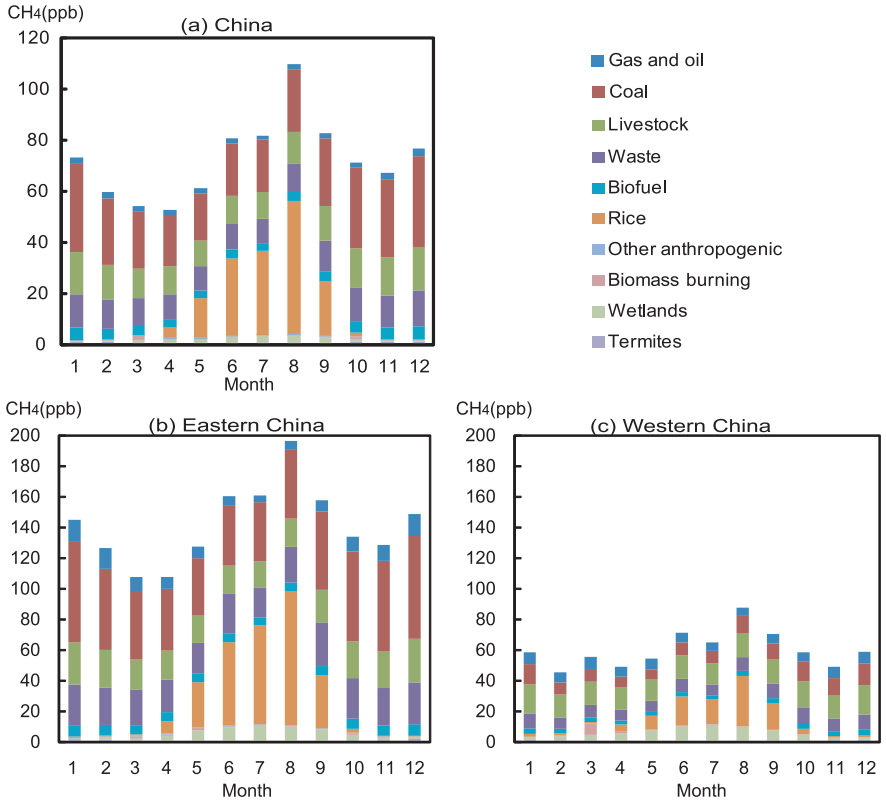

Fig. 9. Simulated monthly mean contributions from individual domestic sources to surface-layer CH_4 concentrations based on tagged simulations: (a) whole of China; (b) eastern China (east of 110°E); (c) western China (west of 110°E).

occurs in March, perhaps indicating the biomass burning before spring plowing in China (Zheng et al., 2005). Wetlands emissions are sensitive to temperature and soil moisture, with their largest emissions in summer and lowest values in winter (Ding et al., 2004) and an annual mean contribution of about 1.5 ppb to the CH_4 concentration. The simulated monthly averaged contributions from domestic sources to surface-layer CH_4 concentration are also shown for eastern China (Fig. 9b) and western China (Fig. 9c). The contributions from domestic sources are generally higher in eastern China than in western China, except for wetlands and biomass burning which have large emissions in western China. The domestic sources that have large impacts on local CH_4 concentrations in eastern China are coal mining (37–67 ppb), waste (19–29 ppb), and rice cultivation (0.3–88 ppb), while in western China the largest impacts are from livestock (14–19 ppb), coal (7–13 ppb), and rice cultivation (0.8–33 ppb).

6. Conclusions

We used the global atmospheric chemical transport model, GEOS-Chem, to investigate the spatial and temporal variations of atmospheric CH_4 over China and quantify the impacts of overseas transport and individual domestic sources on concentrations and seasonal variations of CH_4 over China. Simulated surface-layer CH_4 concentrations over eastern China peak in the summer when biogenic emissions such as rice cultivation are largest because of the warmer temperatures. The annual mean concentrations of CH_4 range from 1800 ppb in western China to 2300 ppb over the more populated eastern China, indicating the influence of anthropogenic emissions.

The foreign emissions of CH_4 were found to have large impacts on CH_4 concentrations over China. Considering the ratios of CH_4 concentrations simulated with foreign emissions only to those with global emissions, the annual and regional mean ratio is 85% in western China (west of 110°E) and 80% in eastern China (east of 110°E), and the ratios peak in spring as a result of the prevailing westerlies in this season and minimize in summer owing to the strong local emissions and the fast removal by OH. Locally, foreign emissions have the highest annual mean contribution of 86% to CH_4 concentration over the Tibetan Plateau and the lowest contribution of about 72% over Shandong and Anhui provinces in eastern China.

We conducted tagged simulation to quantify the monthly contribution from each domestic source to the surface-layer CH_4 concentrations over China. Model results showed that coal mining, livestock, and waste are the major contributors to the monthly contributions from all domestic emissions (MCADE), with annual mean contributions of 36%, 18%, and 16%, respectively. These sources make large contributions to CH_4 concentrations in winter because of weak removal by OH. The influence from rice cultivation is largest in the summer, contributing 52 ppb ($\sim$ 47%) to MCADE in this season. Emissions from rice cultivation are hence the reasons for the observed maximum CH_4 concentrations in summer over eastern China.

Acknowledgements. This work was supported by the Chinese Academy of Sciences Strategic Priority Research Program (Grant No. XDA05100503), the National Natural Science Foundation of China (Grant Nos. 40825016 and 41021004). The authors thank Annemarie FRASER at the University of Edinburgh for providing the initial restart files.

REFERENCES

Ding, W. X., Z. C. Cai, and D. X. Wang, 2004: Preliminary budget of methane emissions from natural wetlands in China. *Atmos. Environ.*, **38**, 751–759.

Dlugokencky, E. J., P. M. Lang, A. M. Crotwell, and K. A. Masarie, 2012: Atmospheric methane dry air mole fractions from the NOAA/ESRL carbon cycle cooperative global air sampling network, 1983–2011. Version: 2012-09-24. [Available online at ftp://ftp.cmdl.noaa.gov/ccg/ch4/flask/ event/.]

Duncan, B., D. Portman, I. Bey, and C. Spivakovsky, 2000: Parameterization of OH for efficient computation in chemical tracer models. *J. Geophys. Res.*, **105**, 12259–12262.

EDGAR v4.0, 2009: European Commission, Joint Research Centre (JRC)/Netherlands Environmental Assessment Agency (PBL). Emission Database for Global Atmospheric Research (EDGAR), release version 4.0. [Available online at http://edgar.jrc.ec.europa.eu.]

Fang, S. X., L. X. Zhou, L. Xu, B. Yao, L. X. Liu, L. J. Xia, and H. Y. Wang, 2012: CH_4 concentrations and the variation characteristics at the four WMO/GAW background stations in China. *Environmental Science*, **33**(9), 2917–2923. (in Chinese)

Fiore, A. M., D. J. Jacob, B. D. Field, D. G. Streets, S. D. Fernandes, and C. Jang, 2002: Linking ozone pollution and climate change: The case for controlling methane. *Geophys. Res. Lett.*, **29**(19), 1919, doi: 10.1029/2002GL015601.

Fiore, A. M., D. J. Jacob, H. Liu, R. M. Yantosca, T. D. Fairlie, and Q. Li, 2003: Variability in surface ozone background over the United States: Implications for air quality policy. *J. Geophys. Res.*, **108**(D24), 4787, doi: 10.1029/2003JD003855.

Frankenberg, C., and Coauthors, 2006: Satellite chartography of atmospheric methane from SCIAMACHY on board ENVISAT: Analysis of the years 2003 and 2004. *J. Geophys. Res.*, **111**, D07303, doi: 10.1029/2005JD006235.

Fraser, A., C. C. Miller, P. I. Palmer, N. M. Deutscher, N. B. Jones, and D. W. T. Griffith, 2011: The Australian methane budget: Interpreting surface and train-borne measurements using a chemistry transport model. *J. Geophys. Res.*, **116**, D20306, doi: 10.1029/2011JD015964.

Fung, I., J. John, J. Lerner, E. Matthews, M. Prather, L. P. Steele, and P. J. Fraser, 1991: Three-dimensional model synthesis of the global methane cycle. *J. Geophys. Res.*, **96**(D7), 13033–13065, doi: 10.1029/91JD01247.

Holzer, M., T. M. Hall, and R. B. Stull, 2005: Seasonality and weather-driven variability of transpacific transport. *J. Geophys. Res.*, **110**, D23103, doi: 10.1029/2005jd006261.

IPCC, 2007: *Climate Change 2007: The Physical Science Basis. Contribution of Working Group I to the Fourth Assessment Report of the Intergovernmental Panel on Climate Change*, Solomon et al., Eds., Cambridge University Press, Cam-

bridge, United Kingdom and New York, NY, USA, 996 pp.

Jacob, D. J., and Coauthors, 2003: Transport and Chemical Evolution over the Pacific (TRACE-P) aircraft mission: Design, execution, and first results. *J. Geophys. Res.*, **108**, D209000, doi: 10.1029/2002JD003276.

Ji, X. Y., L. Y. Yang, Y. S. Wang, and G. B. Cui, 2006: Background density characteristic of the main greenhouse gas near-surface in Tai Lake basin. *The Administration and Technique of Environmental Monitoring*, **18**(3), 11–15. (in Chinese)

Liu, L. X., L. X. Zhou, M. Wen, F. Zhang, S. X. Fang, and B. Yao, 2009: Characteristics of atmospheric CH_4concentration variations at four national baseline observatories in China. *Advances in Climate Change Research*, **5**(5), 285–290.

Pickett-Heaps, C. A., and Coauthors, 2011: Magnitude and seasonality of wetland methane emissions from the Hudson Bay Lowlands (Canada). *Atmos. Chem. Phys.*, **11**, 3773–3779, doi: 10.5194/acp-11-3773-2011.

Prinn, R. G., and Coauthors, 2005: Evidence for variability of atmospheric hydroxyl radicals over the past quarter century. *Geophys. Res. Lett.*, **32**, L07809, doi: 10.1029/2004GL022228.

Schneising, O., M. Buchwitz, J. P. Burrows, H. Bovensmann, P. Bergamaschi, and W. Peters, 2009: Three years of greenhouse gas column-averaged dry air mole fractions retrieved from satellite—Part 2: Methane. *Atmos. Chem. Phys.*, **9**, 443–465, doi: 10.5194/acp-9-443-2009.

Shangguan, X. J., M. X. Wang, D. Z. Chen, and R. X. Shen, 1993: The transport of methane in the rice paddy fields. *Adv. Earth Sci.*, **8**(5), 13–22. (in Chinese)

Streets, D. G., and Coauthors, 2003: An inventory of gaseous and primary aerosol emissions in Asia in the year 2000. *J. Geophys. Res.*, **108**(D21), 8809, doi: 10.1029/2002JD003093.

Su, M. F., Y. P. Lin, X. Q. Fan, L. Peng, and C. S. Zhao, 2012: Impacts of global emissions of CO, NO_x, and CH_4 on China tropospheric hydroxyl free radicals. *Adv. Atmos. Sci.*, **29**(4), 838–854, doi:10.1007/s00376-012-1229-2.

van der Werf, G. R., J. T. Randerson, L. Giglio, G. J. Collatz, P. S. Kasibhatla, and A. F. Arellano Jr., 2006: Interannual variability in global biomass burning emissions from 1997 to 2004. *Atmos. Chem. Phys.*, **6**, 3423–3441, doi: 10.5194/acp-6-3423-2006.

Wang, J. S., J. A. Logan, M. B. McElroy, B. N. Duncan, I. A. Megretskaia, and R. M. Yantosca, 2004: A 3-D model analysis of the slowdown and interannual variability in the methane growth rate from 1988 to 1997. *Global Biogeochemical Cycles*, **18**, GB3011, doi: 10.1029/2003GB002180.

Wang, Y. S., and M. X. Wang, 2000: Seasonal variation and trend of atmospheric methane in Beijing. *Chinese J. Atmos. Sci.*, **24**(2), 157–164. (in Chinese)

Wang, Y. S., and Y. H. Wang, 2003: Quick measurement of CH_4, CO_2 and N_2O emissions from a short-plant ecosystem. *Adv. Atmos. Sci.*, **20**(5), 842–844.

Xiao, Y. P., and Coauthors, 2004: Constraints on Asian and European sources of methane from CH_4-C_2H_6-CO correlations in Asian outflow. *J. Geophys. Res.*, **109**, D15S16, doi: 10.1029/2003JD004475.

Xiong X., S. Houweling, J. Wei, E. Maddy, F. Sun, and C. Barnet, 2009: Methane plume over south Asia during the monsoon season: Satellite observation and model simulation. *Atmos. Chem. Phys.*, **9**, 783–794.

Yan, X. Y., Z. C. Cai, T. Ohara, and H. Akimoto, 2003: Methane emission from rice fields in mainland China: Amount and seasonal and spatial distribution. *J. Geophys. Res.*, **108**(D16), 4505, doi: 10.1029/2002JD003182.

Yevich, R., and J. A. Logan, 2003: An assessment of biofuel use and burning of agricultural waste in the developing world. *Global Biogeochemical Cycles*, **17**(4), 1095, doi: 10.1029/2002GB001952.

Zhang, B., and G. Q. Chen, 2010: Methane emissions by Chinese economy: Inventory and embodiment analysis. *Energy Policy*, **38**, 4304–4316.

Zhang, X. Y., W. G. Bai, P. Zhang, and W. H. Wang, 2011a: Spatiotemporal variations in mid-upper tropospheric methane over China from satellite observations. *Chinese Sci. Bull.*, **56**, 2804–2811. (in Chinese)

Zhang, X. Y, H. Jiang, Y. Q. Wang, Y. Han, M. Buchwitz, O. Schneising, and J. P. Burrows, 2011b: Spatial variations of atmospheric methane concentrations in China. *Inter. J. Remote Sens.*, **32**(3), 833–847.

Zheng, X. Y., C. D. Liu, F. H. Zhao, F. K. Duan, T. Yu, and H. Cachier, 2005: Seasonal characterizers of contributions from biomass burning emissions to atmospheric particles in Beijing. *Scientia Sinica Chimica*, **35**(4), 346–352. (in Chinese)

Zhou, J. B., M. M. Jiang, and G. Q. Chen, 2007a: Estimation of methane and nitrous oxide emission from livestock and poultry in China during 1949–2003. *Energy Policy*, **35**(7), 3759–3767.

Zhou, L. X., D. E. J. Worthy, P. M. Lang, M. K. Ernst, X. C. Zhang, Y. P. Wen, and J. L. Li, 2004: Ten years of atmospheric methane observations at a high elevation site in Western China. *Atmos. Environ.*, **38**(40), 7041–7054.

Zhou, L. X., X. J. Zhou, X. C. Zhang, Y. P. Wen, and P. Yan, 2007b: Progress in the study of background greenhouse gases at Waliguan observatory. *Acta Meteorologica Sinica*, **65**(3), 458–468. (in Chinese)